Applied Energy 413 (2026) 127759

Contents lists available at ScienceDirect

Applied Energy

journal homepage: www.elsevier.com/locate/apenergy

Techno-economic optimization of a modular PEM electrolysis system for distributed hydrogen production

Jie Yang [a], Jichong Yang [a], Ke Chang [a], Chengcheng Lyu [b], Haoming Ma [c], Qiang Cheng [a,*], Zixue Luo [a,*]

[a] State Key Laboratory of Coal Combustion, School of Energy and Power Engineering, Huazhong University of Science and Technology, Wuhan 430074, Hubei, China
[b] Department of Civil and Architectural Engineering and Construction Management, University of Wyoming, Laramie, WY 82071, USA
[c] School of Energy Resources, University of Wyoming, Laramie, WY 82071, USA

HIGHLIGHTS

- Capital expenditure savings of USD 400k are achieved with the modular PEME system.
- Transportation costs of USD 157k are incurred with system relocation.
- LCOH of USD 2.92 per kg is achieved under the grid-connected wind power scheme.
- PV–WT gives lowest off-grid LCOH; WT lowest on-grid LCOH.

ARTICLE INFO

Keywords:
Distributed hydrogen production
PEM electrolysis
Renewable energy
Techno-economic
Monte-Carlo simulation method
Optimization

ABSTRACT

The accelerating deployment of renewable energy systems has intensified interest in green hydrogen as a flexible, low-carbon energy carrier, yet high capital costs (CAPEX) and exposure to renewable intermittency continue to constrain the economic viability of centralized hydrogen production. Here we present a modular, mobile 25-kW truck-deployable proton exchange membrane electrolysis (PEME) system designed to enable flexible, distributed hydrogen generation under variable renewable electricity supply. We develop a system-level techno-economic framework that integrates capacity configuration, renewable coupling, transportation impacts, and uncertainty analysis across six energy supply configurations. Our results show that modular deployment can substantially reduce upfront CAPEX requirements by ~USD 400k or RMB 2.62 million through reduced land use, site development, and installation costs. Among the evaluated configurations, hybrid PV–WT supply achieves the lowest levelized cost of hydrogen (LCOH) under off-grid operation (USD 3.55 or 25.17 RMB per kg), while grid-connected WT electricity yields the lowest LCOH overall (USD 2.92 or 20.55 RMB per kg). Sensitivity and Monte Carlo uncertainty analyses reveal that LCOH is dominated by electrolyzer and renewable generation and are strongly influenced by the stability of renewable electricity supply. These findings demonstrate that modular PEM electrolysis can deliver cost-competitive and deployment-flexible hydrogen production in resource-rich but infrastructure-limited regions, providing a quantitative basis for designing distributed green hydrogen systems that reduce investment risk.

1. Introduction

Hydrogen (H_2) is emerging as a critical low-carbon energy carrier capable of enhancing the efficiency and reliability of renewable energy systems by converting surplus or curtailed solar and wind electricity into a storable, dispatchable fuel [1–4]. Global momentum around green hydrogen is accelerating, as the International Energy Agency (IEA) project that global hydrogen demand will increase from ~100 Mt. today to ~400 Mt. by 2050 under a net-zero scenario, supported by rapidly growing investment that exceeded USD 7.9 billion in 2025, nearly doubling compared to 2024 [5,6]. Yet the cost of green hydrogen, currently estimating at 3.5–6.5 USD/kg [7], remains substantially higher than that of blue hydrogen (2.0–3.5 USD/kg), predominately due to the high capital expenditure (CAPEX) associated with electrolyzer [8]. Moreover, project economics are exposed to the inherent variability

* Corresponding authors.
E-mail addresses: chengqiang@mail.hust.edu.cn (Q. Cheng), luozixue@hust.edu.cn (Z. Luo).

https://doi.org/10.1016/j.apenergy.2026.127759
Received 17 December 2025; Received in revised form 8 March 2026; Accepted 21 March 2026
Available online 30 March 2026

Nomenclature

a	Annual operating and maintenance cost per kW (RMB/kW)
AC	Annual operating and maintenance cost (RMB/year)
BoP	Balance-of-plant
c	Investment cost per kW (RMB/kW)
d	Transportation distance (km)
ELK	Electrolyzer
ε	Efficiency (%)
G	Global irradiance (Wh/m^2)
HHV	Higher heating value (kWh/kg)
IC	Investment cost (RMB)
i	Discount rate (%)
LCOE	Levelized cost of renewable energy (RMB/kWh)
LCOH	Levelized cost of hydrogen (RMB/kg)
M	Amount of hydrogen generated annually (kg/year)
m	Mass flow rate of produced hydrogen (kg/h)
P	Power (W)
ρ	Power input coefficient
PC	Penalty cost (RMB)
PEME	Proton exchange membrane electrolysis
PV	Photovoltaic plant
RC	Replacement cost (RMB)
r	Replacement cost per kW (RMB/kW)
SC	Electricity sales revenue (RMB)
TC	Transportation cost (RMB)
TEMP	Temperature (°C)
v	Wind speed (m/s)
WT	Wind turbine

and seasonality of renewable resources; when wind or solar output falls below expectations, electrolyzers operate far below nameplate capacity, driving up the levelized cost of hydrogen (LCOH) and elevating investment risk [9]. These challenges underscore the need for system configurations that can mitigate renewable intermittency and de-risk project lifetimes, motivating increasing interest in distributed, modular hydrogen production systems that can scale flexibly with local resource availability.

Among commercially available electrolyzer technologies (TRL 7–9), proton-exchange-membrane electrolysis (PEME) offers compact system architecture, fast dynamic response, and high operating pressures [10–13], making it particularly well suited for modular and distributed hydrogen production compared with conventional alkaline systems [14,15]. Modular PEME configurations provide the operational flexibility (e.g., small, integrable and transportable) that centralized plants cannot achieve, enabling hydrogen production to better follow variable renewable supply, reduce curtailment, and improve asset utilization, particularly in rural and remote regions, thereby enhancing the renewable electricity production while lowering overall costs [16–18]. Yet despite growing interest in modular designs, the cost structure, scaling behavior, and techno-economic trade-offs of PEM-based modular hydrogen systems remain poorly quantified, leaving a critical knowledge gap in widely deploying the distributed hydrogen production systems though optimized system design to mitigate intermittency-driven risks [19–22].

Recent work has advanced water electrolysis for renewable-powered hydrogen production in three directions [23–26]. For fluctuating PV supply, a modular proton-exchange-membrane electrolysis (PEME) energy-management framework based on constrained nonlinear optimization combined with RPAS has been proposed to coordinate multi-stack power allocation and improve efficiency/hydrogen yield while mitigating uneven utilization and degradation. Second, studies comparing single-stack and modular systems with PV forecasting and power allocation report that modular configurations can substantially increase annual hydrogen production and reduce voltage-decay-related degradation, while noting remaining uncertainties in degradation attribution/estimation. Finally, modeling benchmarks suggest grey-box PEME models often provide a practical accuracy–complexity trade-off for energy-management applications, and emphasize that no single model is optimal across all operating regimes. Existing studies have conducted the techno-economic analysis (TEA) of modular PEM electrolysis with primary focus through operational flexibility and system integration perspectives [27–29]. For example, El-Hamalawy et al. showed that independently controlled PEM modules can improve renewable coupling efficiency and reduce hydrogen lifecycle costs, but the analysis relies on assumed stack cost and lifetime parameters and does not investigate module sizing, scaling behavior, or distributed deployment [18]. Zheng et al. demonstrated that module-level load sharing under fluctuating renewable conditions can reduce hydrogen production costs; however, the study focuses on operational strategies for a single configuration and does not reflect design-level optimization or scalability [30]. Henkel et al. proposed a modular electrolysis plant coordinated by a multi-agent system to enhance flexibility and resilience, yet reported only relative economic effects without explicit CAPEX, OPEX, or levelized hydrogen cost estimates [31]. At the system level, Evro et al. assessed green hydrogen integration within distributed energy systems but treated electrolyzers as aggregated assets and did not resolve the techno-economic impacts of module size, quantity, or multi-stack PEM configurations [32].

Additionally, the limited understanding of cost-reduction potentials and techno-economic optimization strategies further constrains the development of modular electrolyzer systems [33,34]. Zheng et al. proposed a power allocation strategy for modular electrolyzer systems that maximizes overall techno-economic performance by integrating efficiency modeling with degradation factor considerations; however, their optimization remains confined to fixed operating conditions and does not incorporate broader system-level cost trade-offs or dynamic market factors [35]. Wang et al. proposed a two-stage control strategy that enhances renewable energy utilization while extending the service life of electrolyzers. The approach primarily focuses on operational scheduling and does not extend to comprehensive techno-economic assessments, such as long-term degradation cost modeling or stack replacement cost-benefit analysis [28]. Therefore, the research remains confined to short-term performance metrics, exhibiting shortcomings in life-cycle cost modeling, scalability analysis, and economic risk assessment [36].

Building on these insights, this study addresses several system-level questions that remain largely unexplored in existing literature. First, we examine how modular PEM electrolysis (PEME) architectures can reduce capital expenditure through scalable deployment, improved capacity utilization, and more efficient alignment with variable renewable resources. Second, we evaluate whether additional costs introduced by modularity, such as module transportation, integration and site installation, offset or outweigh the potential economic benefits. Third, we identify the key technical and economic drivers that shape the performance of modular PEM systems and develop an optimization framework to quantify their influence on levelized hydrogen cost and project risk. Together, these analyses provide the first integrated assessment of how modular PEM electrolysis can be configured and optimized to achieve cost-effective, renewable-integrated hydrogen production, addressing critical gaps not yet resolved by the current body of research.

In this study, we develop and evaluate a 25-kW modular PEME system designed for truck-mounted deployment, enabling flexible off-grid operation and relocatable hydrogen production. We developed a techno-economic model to quantify the levelized cost of hydrogen (LCOH) under both off-grid renewable and grid-connected electricity scenarios and established a particle-swarm optimization (PSO) scheme coupled with Monte Carlo uncertainty analysis to identify cost drivers and assess system robustness. Our results indicate that modular deployment can substantially reduce capital investment: a 25-kW distributed/mobile configuration can decrease total capital expenditures by about RMB 2.62 million (or USD 370k) through savings in construction, equipment installation, station development and land use. Although system relocation introduces increasing transportation costs, the modular architecture still delivers lower LCOH (USD 2.91–3.67 or RMB 20.55–25.91 per kg) in both grid-connected and renewable-powered cases. Sensitivity and uncertainty analyses highlight the decision-making factors in LCOH for the proposed PEME system. Collectively, these findings provide a quantitative foundation for designing and optimizing distributed modular electrolyzer systems, offering actionable insights for reducing investment risk and accelerating the commercial deployment of distributed green hydrogen infrastructure.

2. Material and methods

2.1. Modular PEME configuration

The modular PEME system is mobile and easily integrable, enabling hydrogen production in rural or remote regions that lack grid electricity but possess otherwise unutilized local wind or solar resources. Its transportable architecture eliminates the need for permanent site preparation and fixed infrastructure, thereby reducing CAPEX associated with land development, construction, and large-scale balance-of-plant (BoP) installation. By allowing a single unit to be redeployed across multiple locations, the modular system further amortizes equipment costs while matching production capacity to local hydrogen demand and renewable resource availability. This flexible configuration

Fig. 1. Modular PEME hydrogen production system: (a) 25-kW PEME electrolyzer, (b) pure water machine, (c) chiller.

supports scalable deployment pathways that differ fundamentally from centralized electrolysis plants, which typically require substantial upfront investments in stack capacity, extensive balance-of-plant systems, and on-site installation. Models for PV, wind turbine, hydrogen storage, and battery subsystems are provided in Supplementary Information Section A.

Fig. 1 presents a 25-kW PEME hydrogen production system, which consists of a PEME stack (Fig. 1a) integrated with auxiliary equipment, including a purified water unit (Fig. 1b) and a chiller (Fig. 1c). The water purification process treats the raw water to deionized water with a conductivity of less than 0.1 μS/cm, which subsequently feed into the electrolyzer. The chiller regulates the equipment temperature during H_2 production, which requires the cooling water pressure at 0.2–0.3 MPa, flow rate greater than 4.3 m^3/h, and temperature between 25 and 30 °C. The system produces 5 Nm^3/h gas with power consumption of 25-kW. In this study, the rated hydrogen production of the 25-KW integrated PEM electrolyzer module is reported as 5 Nm^3/h, where Nm^3 is defined at 0 °C and 1 atm. To align with the mass-based techno-economic analysis, we also provide the mass-flow equivalence: at 0 °C and 1 atm, the hydrogen density can be approximated as 0.0899 kg/Nm^3, and thus 5 Nm^3/h corresponds to about 0.45 kg/h. Unless explicitly stated, system-level supply-demand accounting, cost calculations, and penalty terms are implemented in kg/h throughout this study.

Fig. 2 is the process flow chart of the proposed modular PEME system. The system encompasses pure-water tank, PEME stack, power supply, water tank, circulating water pump, gas-water separator, purification system. Appropriate sensors are configured on the periphery to monitor each link in real time to achieve the purpose of producing qualified hydrogen. After the qualified deionized water from the periphery enters the built-in water tank, the system judges the water level and water temperature. When the water level in the water tank rises to the set position, the equipment starts to run. The water in the water tank is pumped into the electrolyzer through a circulating pump. The water is electrolyzed by the current in the electrolyzer, and a chemical reaction occurs inside the electrolyzer to generate hydrogen and oxygen. The hydrogen, oxygen and water return to the water tank, and the hydrogen enters the gas-water separator for water-gas separation. The oxygen in the water tank is removed from the outside by the oxygen extraction fan, and the water continues to be circulated and electrolyzed again. The hydrogen entering the gas-water separator, after the first stage of separation, enters the purification system for ultimate purification. The purification system adopts the PSA pressure swing adsorption principle. When the purification tank A is working, the purification tank B will be regenerated and switched at regular intervals. In this process, a small amount of dry hydrogen is used to purge the reproduction cylinder to remove moisture from the reproduction cylinder.

2.2. D/MHS efficiency model

The system adopts PLC intelligent control system, which manages all operational parameters of the system and monitors the real-time temperature, current, voltage, working pressure, hydrogen production rate and other parameters of the electrolyzer stack of the hydrogen production unit in real time, and monitor the condition status of the electrolyzer according to various parameters at any time. After pressing the start button, the equipment will enter the emptying stage, which lasts for 180 s. At this time, the hydrogen production equipment electrolyzes a small amount of gas, and the gas production rate is 30%–70% of the maximum hydrogen production, and the remaining air in the hydrogen production system is discharged out of the system. The electrolysis current can be adjusted in the user interface to monitor the hydrogen production efficiency of the electrolyzer under different power inputs, and the test safety upper limit is 450 A. Set the upper limit of electrolysis pressure to 2 MPa and the upper limit of working temperature to 45 °C. The water flow rate was set at 3 m^3/h. Simulate fluctuating power inputs (gradual increase, decrease, and random changes) in different modes, adjust the current within the range of 100 A to 450 A, and control the back pressure valve to stabilize the working pressure at approximately 2 MPa.

The electrolyzer model used in this study is an empirical model based on experimental data fitting. The dynamic efficiency of PEME electrolyzer under different loads are calculated as follows [2]:

$$\rho = \frac{P_{\mathrm{ELK}}}{P_{\mathrm{ELK,R}}} \tag{1}$$

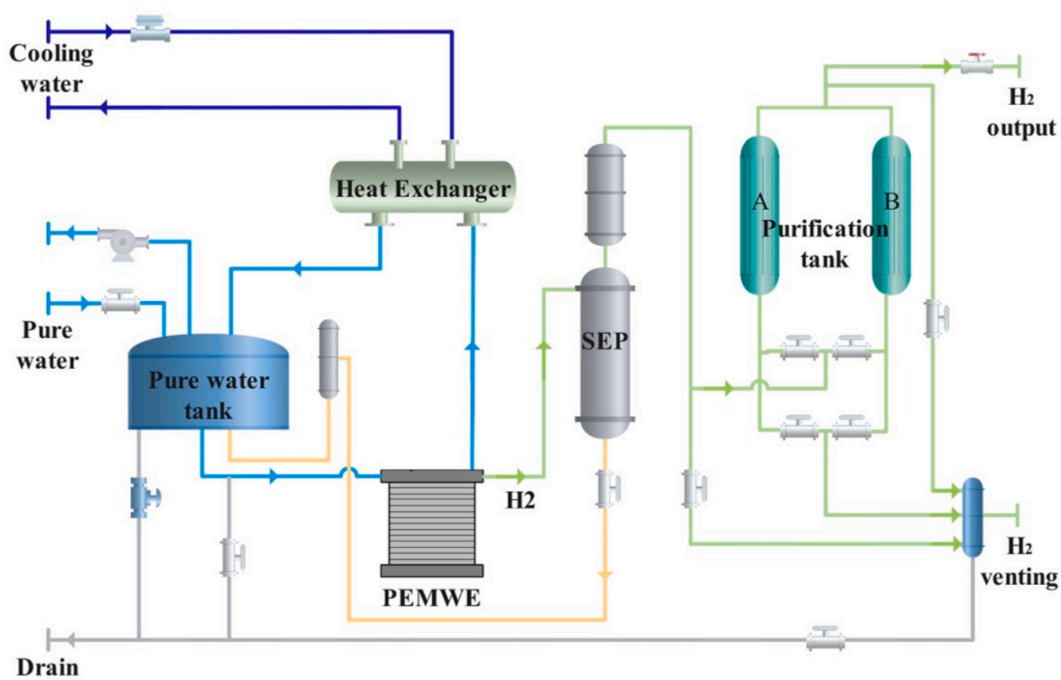

Fig. 2. Process flow chart of the hydrogen production system.

$$\varepsilon_{ELK} = C_1\rho^3 + C_2\rho^2 + C_3\rho + C_4 \tag{2}$$

where P_{ELK} and $P_{ELK,\ R}$ indicate the current and rated input power, ρ is the power input coefficient, and ε_{ELK} is the electrolyzer efficiency. The corresponding hydrogen output rate can be calculated as follow [37]:

$$m_{H_2,ELK} = \frac{P_{ELK}\varepsilon_{ELK}}{HHV_{H_2}} \tag{3}$$

where $m_{H_2,ELK}$ is the mass flow rate of produced hydrogen; HHV_{H_2} is the higher heating value of hydrogen, which equals 39.7 kWh/kg.

Fig. 3 shows the fitting results based on the experiment. Owing to the favorable transient response and operational stability of the PEME electrolyzer, under the set general working conditions (2 MPa, 45 °C, 3 m^3/h), when the input power fluctuated, the three groups of experimental results were similar. Fig. 3(a) shows the relationship between electrolysis efficiency and input power coefficient obtained by fitting experimental data. When the input power is 20% of the nominal power, the electrolysis efficiency is 89.36%, and it decreases with the increase of input power. When the system works at rated power, the electrolysis efficiency drops to 74.69%. When the electrolysis device is overclocked, the electrolysis efficiency decreases faster, and the electrolysis efficiency is as low as 70% when the power input coefficient is 1.16. Fig. 3(b) shows the hydrogen production rate calculated using the fitting results and compared with the experimental results. The MATLAB fitting tool was employed, yielding an R^2 value of 0.9988 and an RMSE of 0.0014. The effective range spans a power input coefficient from 19.62% to 116.00%. The underlying experimental dataset are presented in Table S1 of the Supplementary Information. The PEME efficiency model obtained based on experimental data fitting is as follows:

$$\varepsilon_{ELK} = -0.1458 \cdot \rho^3 + 0.2925 \cdot \rho^2 - 0.3536 \cdot \rho + 0.9517 \tag{4}$$

2.3. Techno-economic analysis

Compared to conventional centralized hydrogen production systems, the integrated PEME system reduces capital expenditures (IC_{save}) for hydrogen stations, primarily in land use (IC_{land}), construction costs ($IC_{construction}$) and installation costs ($IC_{installation}$). However, it also incurs certain transportation costs (TC) during equipment relocation.

$$IC_{save} = IC_{land} + IC_{construction} + IC_{installation} \tag{5}$$

$$TC = n_{transporation} \cdot (d \cdot TC_{base} + TC_{labor}) \cdot \frac{P_{ELK,R}}{P_{ELK,base}} \tag{6}$$

$n_{transportation}$ is the number of equipment transports within the design life span; d is the transport distance, km; TC_{base} is the single-vehicle transport cost per trip, RMB/km; TC_{labor} is a single integrated unit for labor costs in a single scheduling cycle, RMB; $P_{ELK,\ base}$ is the capacity of a single integrated unit, 25-kW.

LCOH serves as an indicator for assessing the economic feasibility of hydrogen production, and is calculated as follows [38,39]:

$$LCOH = \frac{IC + \sum_{t=1}^{N}\frac{AC}{(1+i)^t} + \sum_{n_R}\frac{RC}{(1+i)^{t_R}} + \sum_{t=1}^{N}\frac{PC}{(1+i)^t} - \sum_{t=1}^{N}\frac{SC}{(1+i)^t}}{\sum_{t=1}^{N}\frac{M_{H_2,ann}}{(1+i)^t}} \tag{7}$$

where IC, AC and RC are the investment, annual operating and maintenance, and replacement costs of system components, including PV plant and wind farm, electrolyzer, hydrogen tank, battery and converter; PC is the penalty costs and includes the cost of wasted electricity during off-grid operation, the cost of purchasing electricity during grid-connected power shortages, and penalty costs incurred due to insufficient hydrogen supply and waste. The penalty costs for electricity can be calculated using the electricity prices at different times. The actual price of green hydrogen may vary across regions, supply chain arrangements, and hydrogen refueling station operational models. In certain areas of China, green hydrogen prices range 29.33–38.13 RMB or USD 4.11–5.33 per kg [40]. Therefore, this paper adopts 35.00 RMB or USD 4.9 per kg as the benchmark value for cross-scenario comparisons. Hydrogen load shall be set at a stable load of 30 kg/h. It should be emphasized that the hydrogen load of 30 kg/h used in the LCOH formulation represents the station-level constant demand in our MW-scale case study [41], rather than the production capacity of a single 25-kW module. Under the same normal-condition definition (0 °C and 1 atm), 30 kg/h is approximately equivalent to 334 Nm^3/h, and meeting this demand typically requires a cluster consisting of multiple 25-kW modules, while the exact requirement may vary with the operating point and power-supply conditions. The number of modules required under different conditions is shown in Table 7. Accordingly, the subsequent evaluations of shortage, curtailment/waste, and penalty cost are all referenced to this station-level demand definition; SC denotes revenue generated through electricity sales; $M_{H_2,ann}$ is the amount of hydrogen generated annually; i is discount rate with a value of 0.08; N is the system design life, here it is 20 years.

2.4. Optimization framework

Combining the renewable energy electricity production system with hydrogen production and energy storage device including electrolyzer and hydrogen tanks can convert renewable energy electricity into hydrogen energy and store it. This is the main way to produce green hydrogen and realize hydrogen energy storage. Layout of a PEME hydrogen production system powered by renewable energy is shown in Fig. 4. The system consists of four modules: electricity production, hydrogen production, energy storage and hydrogen application. Solar and wind energy is used for power production by an external input system, and then the electricity is input into the electrolysis equipment

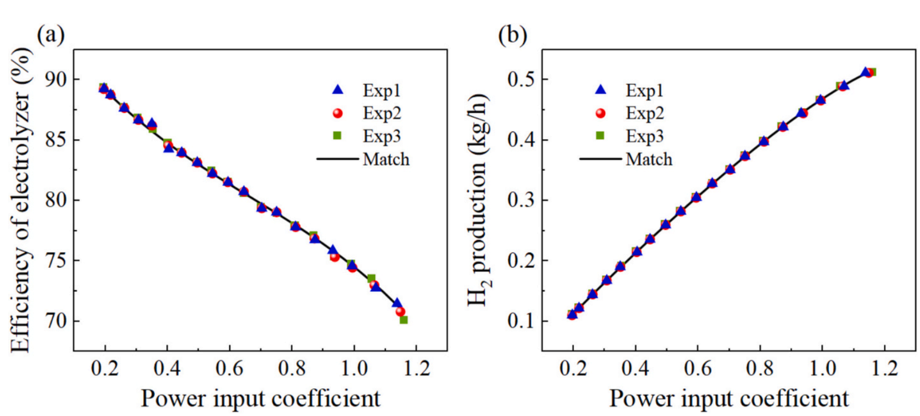

Fig. 3. Fitting results based on experimental data: (a) electrolysis efficiency, (b) H2 production.

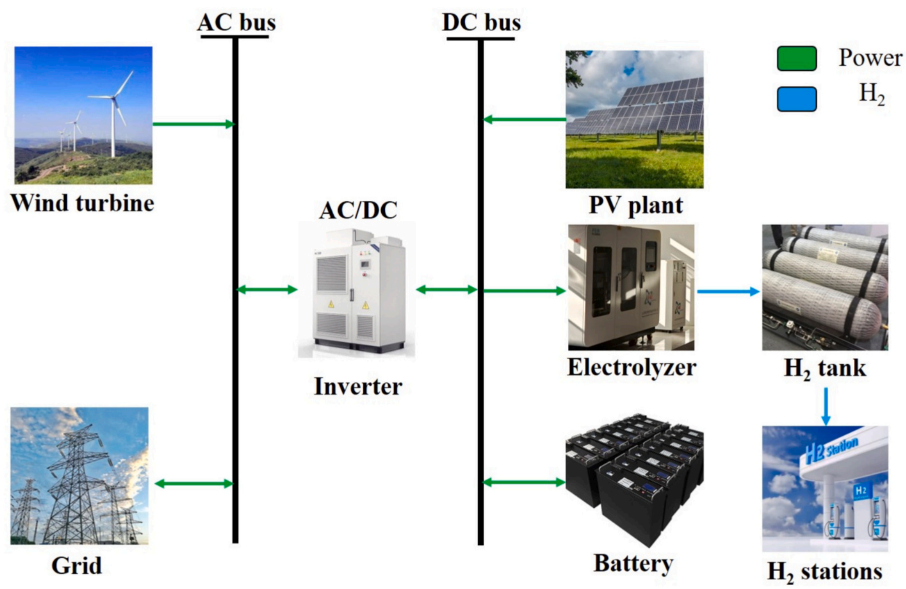

Fig. 4. Layout of a Modular PEME hydrogen production system.

to convert the electricity into hydrogen energy, realizing wind and solar power consumption and green hydrogen preparation. Batteries and hydrogen storage tanks are the allocation devices for electricity and hydrogen. When the WT and PV power production capacity cannot meet the load requirements, the battery can provide dispatchable power supplement. If the battery cannot consume the remaining electricity, power abandonment will occur when off-grid, and electricity will need to be sold to the grid when connected to the grid. The hydrogen tank is used to receive excess hydrogen and adjust the supply according to the hydrogen load demand. Inadequate hydrogen storage capacity may result in supply shortages. PV plant, wind farm, water electrolysis hydrogen production devices, batteries, hydrogen storage tanks and other equipment work together to achieve low-cost green hydrogen preparation and hydrogen supply.

The renewable energy water electrolysis hydrogen production system includes a power plant, electrolysis equipment and energy storage devices. The system operation strategy flow chart is shown in Fig. 5. According to the hydrogen load demand, renewable energy power production, electrolysis device load and energy storage equipment capacity, system operations can be categorized into Scenario (a) and Scenario (b), each containing four cases applicable to both off-grid and grid-connected systems. The detailed descriptions are presented in SI.

Within the optimization and simulation framework, the hydrogen demand profile is consistently implemented in kg/h as the input and constraint basis, and the same unit convention is used in the mismatch and penalty-cost terms. In the base-case scenario, the station-level demand is represented as a constant load (30 kg/h) to highlight how system configuration and energy-supply options influence techno-economic performance; under this setting, all scenario simulations and uncertainty analyses adopt the same demand definition and unit system.

Flowchart of the design optimization of the system as shown in Fig. 6. The installed capacity of the electrolysis device, battery, and hydrogen storage tank was optimized. The LCOH goal was considered in the system optimization process, and the particle swarm optimization algorithm (PSO) was introduced. During the optimization process, the function tolerance is set to 1×10^{-6} and the maximum number of

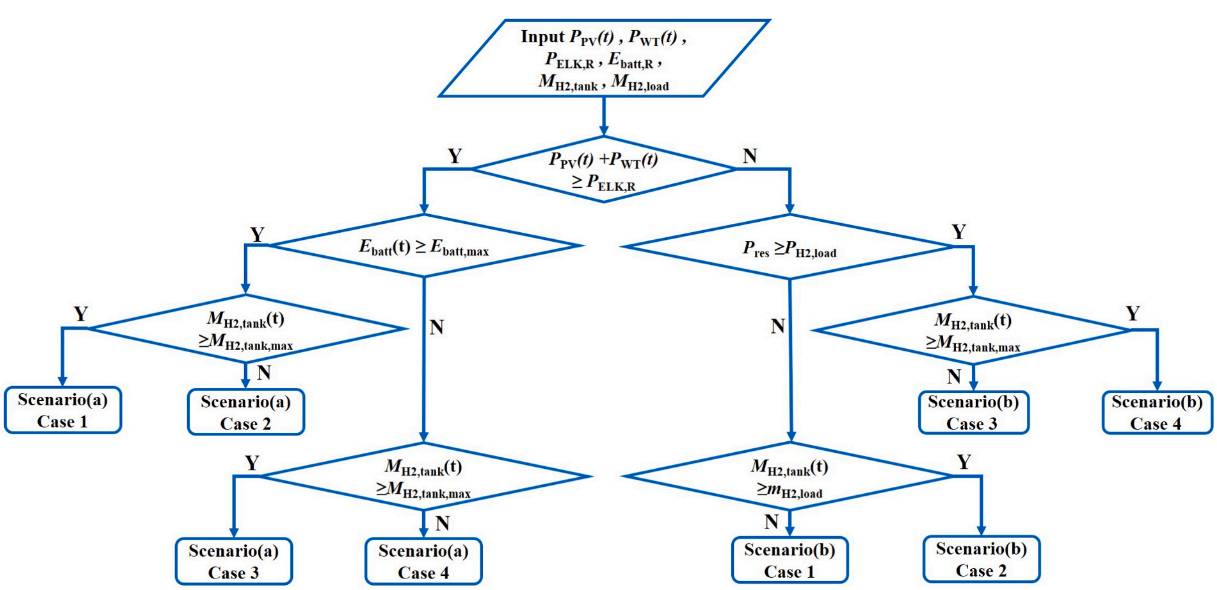

Fig. 5. Flowchart of the operation strategies of the system.

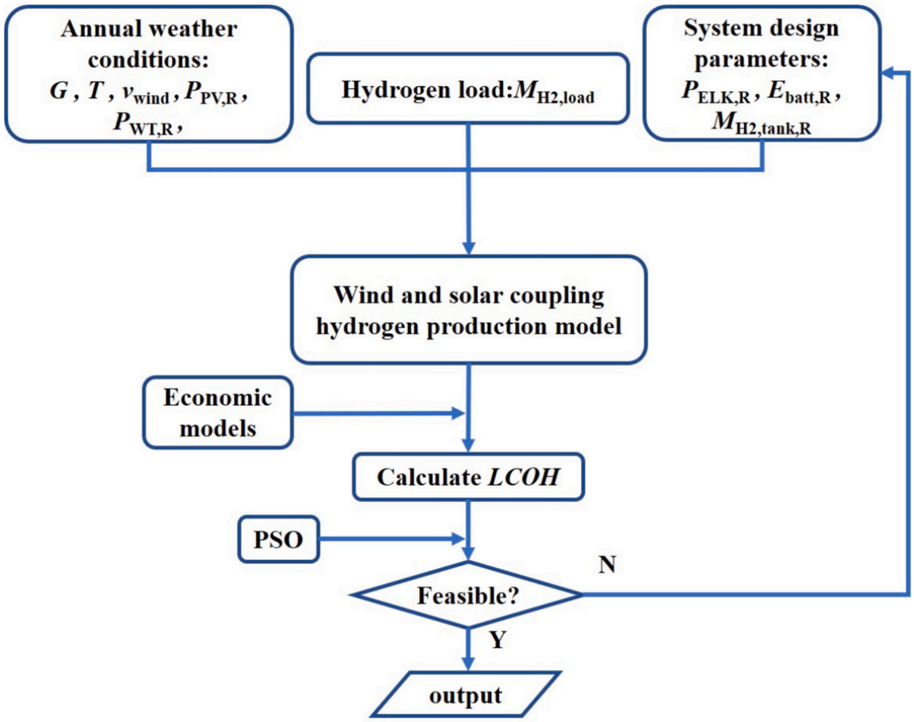

Fig. 6. Flowchart of the design optimization of the system.

iterations is 500.

3. Results

3.1. CAPEX saving

The case study for the water electrolysis system adopts a maximum hydrogen production capacity of 1000 Nm^3/h per unit, with a power requirement not exceeding 6 MW at full load [42]. The estimated land use for a typical hydrogen production station is 6030 m^2. As summarized in Fig. 7 and Table 1, the electrolyzer and hydrogen purification units with essential auxiliaries (pure water supply and chiller) are treated as retained elements because they are integrated into the mobile module.

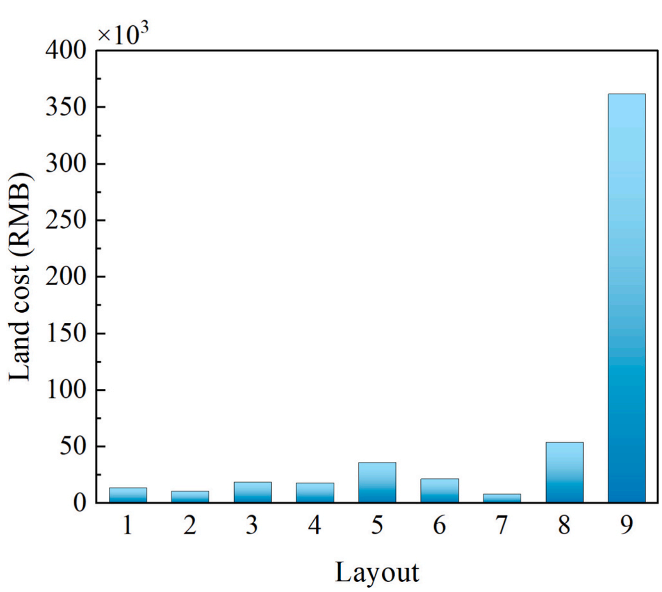

Fig. 7. Land costs for each primary layout.

Table 1
Land use for hydrogen production station [42].

Number	Primary Layout	Land use (m^2)	Land cost (RMB)	Disposal Method
1	Electrolyzer, hydrogen purification equipment	150	13,500	Retained
2	Pure water system, chiller	120	10,800	Retained
3	Hydrogen compressor	210	18,900	Removed
4	Power distribution system, hydrogen production power supply	200	18,000	Removed
5	Cooling towers, heat exchangers	400	36,000	Removed
6	Tube filling and storage	240	21,600	Removed
7	Filling, storage of cylinder assemblies	90	8100	Removed
8	Control room, duty stations, other public areas	600	54,000	Removed
9	Safety distance area, public land, etc.	4020	361,800	Reduced/ Removed
	Total	6030		

In contrast, several fixed-site-dependent infrastructures in a typical hydrogen production station, such as the hydrogen compressor, power distribution system and hydrogen production power supply, cooling towers and heat exchangers, tube filling and storage, filling and storage of cylinder assemblies, and control room and other public areas, are categorized as Removed under mobile deployment, while the safety distance area and public land are categorized as Removed or Reduced. In the subsequent calculations, this item is treated as Removed, as mobile deployment significantly reduces the required safety setback areas and associated public land compared with a conventional fixed station. It should be noted that the hydrogen production equipment itself occupies only a small proportion of the total footprint. Therefore, adjusting hydrogen production capacity or adopting electrolyzers with different power densities will not significantly alter the overall land requirements for the hydrogen production station. When locating hydrogen production stations near wind farms, typical land acquisition costs are approximately 90 RMB or USD 12.60 per m^2. By adopting a modular PEME hydrogen production system, land requirements can be reduced for all components except the electrolyzer, hydrogen purification equipment, pure water system, and refrigeration units. This could reduce the land area required by up to 5760 m^2, saving approximately RMB 0.52 million (or USD 72.80k) in capital expenditures. Table 2 presents the CAPEX saving results. The construction project for this hydrogen station requires RMB 1.62 million (or USD 226.80k), with equipment installation costs totaling RMB 0.48 million (or USD 67.20k) [43]. The total capital expenditure reduction amounts to approximately RMB 2.62 million (or USD 366.80k).

Construction and installation expenditures are project-specific and depend on the detailed design and functional requirements (e.g., the scope of control rooms, offices, and public facilities). Due to data availability constraints, we estimate potentially avoidable incremental construction/installation investments using aggregated literature values and provide a removed-versus-retained mapping. The reported CAPEX savings are therefore scenario-dependent and may be smaller when additional land purchase or extensive site-specific civil works are required. Mobile modular deployment does not imply a zero-requirement site: permitting/safety management and temporary exclusion zones are typically still required. Although safety setback requirements remain applicable, the compact and integrated configuration of the mobile system substantially reduces the required exclusion zone compared with a conventional fixed station. Consequently, the associated land occupation is assumed to be eliminated in the present land cost calculation and is classified as Removed. Essential foundations and mandatory protective arrangements remain necessary, while handling/positioning needs are discussed and accounted for in Section 3.2 Impact of transportation.

3.2. Impact of transportation

Given the high level of integration in the modular configuration, the baseline analysis assumes that recurring site-integration expenditures are minimal and therefore not explicitly itemized. In addition, relocations can be scheduled during off-peak periods and short time windows, such that the effective production downtime is treated as negligible in the baseline case.

Based on existing projects, there are three hydrogen production plants located at sites A, B, and C. The road transport distance d between hydrogen production plants is specified. The transportation impacts in this paper encompass shipping fee between different locations and labor costs incurred during scheduling. The relevant parameters TC_{base}, TC_{labor}, and transport-related parameters of a 25-kW Modular PEME Hydrogen Production System are detailed in Table 3.

As shown in Fig. 8(a), shipping fees vary with transportation frequency, system size and distance between sites. For a 3 MW system scheduled five times over a 20-year lifecycle, the shipping fees for A–B, A–C, and B–C are RMB 0.13, 0.15, and 0.29 million (or USD 18.82k, USD 21.50k and USD 40.32k). Similarly, shipping fees for a 6 MW system double during scheduling. Transportation costs increase with distance and system scale, reflecting higher expenses associated with long-distance shipping and larger equipment. Fig. 8(b) illustrates the labor costs associated with loading, unloading, and handling operations at each transportation site. These labor costs increase proportionally with transportation frequency and system scale. When system capacity is scaled up to 6 MW, labor costs amount to RMB 0.54 million (or USD 75.60k). The cost increase stems from the greater number of handling operations required for larger equipment, while increased transportation frequency further drives up labor expenditures. As discussed for Fig. 8(c), over the design life span, for each installed capacity (3 MW and 6 MW), transportation costs increase with the number of transport trips, resulting in additional transportation costs of up to RMB 1.12 million or USD 156.80k (for equipment with a capacity of 6 MW and 5 dispatch events over a 20-year period). With a transportation frequency maintained at 3 times, equipment capacity set at 3 MW, the transportation costs for A–B, A–C, and B—C are RMB 0.25 million, RMB 0.24 million, and RMB 0.33 million (or USD 35.00k, USD 33.60k and USD 46.20k) respectively. Reducing the number of transport trips effectively controls transportation costs, particularly when scheduling across multiple sites. Transportation costs increase linearly with the installed capacity. While increased system capacity implies greater hydrogen production capability, transportation costs also rise accordingly, necessitating a comprehensive consideration of capacity and transportation costs in project design. Therefore, optimizing transport routes, minimizing the number of trips, and rationally planning the installed capacity are key to reducing overall transportation costs.

Table 2
CAPEX saving.

Item	IC_{land}	$IC_{construction}$	$IC_{installation}$	IC_{save}
Value (million RMB)	0.52	1.62	0.48	2.62

Table 3
Transportation-related parameters.

Item	Value
$n_{transportation}$	1–5
d (km)	
A–B	16
A–C	14
B–C	30
Modular PEME Hydrogen Production System	
Dimensions (m*m*m)	3.0*2.0*1.8
Weight (ton)	0.8
$P_{ELK, base}$ (kW)	25
$P_{ELK, R}$ (MW)	3–6
Transport vehicles	
Dimensions (m*m*m)	3.8*2.4*2.4
Payload (ton)	1.5–2.0
TC_{base} (RMB/km)	16
TC_{labor} (RMB)	450

3.3. Decision variables

In this study, the system design site is located in Wuhan, Hubei Province, China (30.5743N, 114.21114E). The hourly meteorological conditions of Wuhan throughout the year are shown in Fig. 9. Data sourced from NASA's Prediction of Worldwide Energy Resources (POWER). Due to the inherent instability and intermittency of power output from photovoltaic power stations and wind farms, significant challenges arise for grid integration. As a result, grid access is sometimes restricted, and the curtailment rates of both PV and WT remain high. The purpose of hydrogen generation systems powered by renewable energy is to convert electricity into hydrogen for storage and improve resource utilization efficiency.

This study compares the costs of renewable hydrogen generation in off-grid and grid-connected systems under conditions of 10 MW PV, 10 MW WT, and a combination of 5 MW PV and 5 MW WT. Table 4 presents the allowable ranges for installed capacities of the PEME electrolyzer, battery, and hydrogen tank. In grid-connected scenarios, the system enables two-way power exchange with the grid: electricity is purchased from the grid when renewable generation is insufficient and energy storage cannot fully meet operational demands; electricity is sold to the grid when renewable generation exceeds requirements after supplying electrolysis and charging storage. Grid-connected electricity purchase rates follow a time-of-use pricing structure (Table 5): peak hours (8:00–11:00, 18:00–22:00) at 0.974 RMB/kWh or USD 136.36 per MWh, valley hours (23:00–7:00) at 0.318 RMB/kWh or USD 44.52 per MWh, and standard rates of 0.629 RMB/kWh or USD 88.06 per MWh during all other periods [43]. Correspondingly, hourly grid-connected electricity

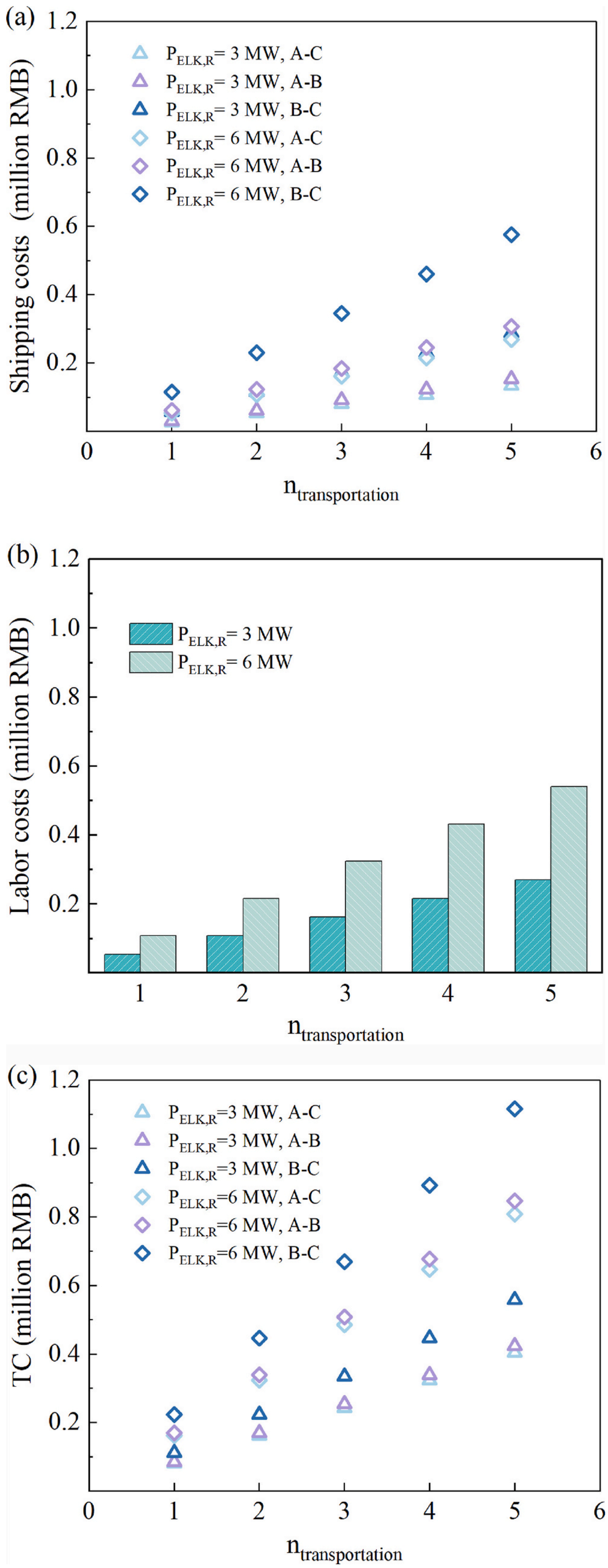

Fig. 8. Transportation-related impacts expressed as TC: (a) shipping fees between sites, (b) labor cost for loading/unloading and handling, (c) total dispatch-induced cost TC (sum of shipping fee and labor cost).

costs/revenues are calculated using the same time-of-use pricing system. Settlement mechanisms may vary across regions; therefore, grid-connected transaction revenues should be interpreted within the context of scenario assumptions. Table 6 presents core cost-related parameters for the system. In this study, electrolyzer investment and replacement costs are computed on a specific-cost basis and scaled by the cluster rated power: $IC_{ELK} = c_{ELK}P_{ELK,R}$, $AC_{ELK} = a_{ELK}P_{ELK,R}$, $RC_{ELK} = r_{ELK}P_{ELK,R}$, where c_{ELK}, a_{ELK} and r_{ELK} represent the investment cost, operating and maintenance cost, and replacement cost per kW of the electrolyzer [41]. The system design cycle is 20 years. As summarized in Table 6, auxiliary and BoP costs are assumed to scale linearly with system capacity. Although partial non-linear scale effects associated with shared equipment may exist, their omission is consistent with the scope of this early-stage techno-economic analysis and is unlikely to change the comparative trends or conclusions presented [44].

3.4. Optimal design

The design parameters of the hydrogen generation system under the two operation strategies of off-grid and grid-connected are optimized. When there is a power shortage, the battery is used for power supply first. Optimization results for the system are shown in Fig. 10. During the optimization process, it was found that the optimized installed capacity of batteries in all scenarios was around 1 MWh. The increase in the installed capacity of energy storage batteries caused an increase in LCOH, and the increase in battery installed capacity caused a decrease in the economic efficiency of the hydrogen generation system. A cost comparison reveals that grid-connected systems offer cheaper hydrogen generation. Under the off-grid scheme, the most economical hydrogen generation from PV-WT power generation is 25.17 RMB/kg (or USD 3.52 per kg); under the grid-connected scheme, the LCOH of hydrogen generation from WT power generation is the lowest, at 20.55 RMB/kg (or USD 2.88 per kg). Under PV design conditions, the off-grid system electrolyzer capacity is 4.86 MW, the hydrogen tank capacity is 770 kg, and the LCOH is 35.11 RMB/kg (USD 4.92 per kg). When the grid-connected solution is adopted, the electrolyzer capacity is significantly reduced, the required capacity of the hydrogen tank is reduced by 270 kg, and the LCOH is reduced to 31.75 RMB/kg (or USD 4.45 per kg). When PV and WT are used in combination for power generation, LCOH decreases by 28.31% and 32.22% compared to photovoltaics, with the significant decrease in electrolyzer capacity (27.25% and 24.68%) playing a dominant role.

To ensure cross-scale consistency, the MW-scale electrolyzer is represented as a cluster of 25-kW base modules operated. The module count is defined as $N_{mod} = \lceil P_{ELK,R}/25\ \mathrm{kW} \rceil$. $P_{ELK,R}$ is the rated power of the MW-scale electrolyzer. Accordingly, 3 MW, 6 MW and 10 MW correspond to approximately 120, 240 and 400 modules, respectively. Table 7 presents key assumptions, optimized dimensions, and grid interactions under different configurations.

With regard to the cost composition, LCOH can be divided into the investment, operation and maintenance and replacement costs of each system component and the penalty costs caused by unstable hydrogen supply, and the power purchase cost and power sales revenue in the grid-connected system. Under different power generation conditions, the hydrogen generation cost components $LCOH_i$ and the levelized cost of electricity (LCOE) of off-grid and grid-connected systems are shown in Fig. 11. The cost of power generation equipment and electrolysis device is the main contributor to the system cost. Under the three power generation modes, the sum of the costs of the two in the off-grid system is 74.77%, 68.55% and 75.49%, and the sum of the costs of the two in the grid-connected system is higher than 80%. In Fig. 11(a), power equipment, electrolyzer and penalty costs are the main contributors to the LCOH of the off-grid system, accounting for about 90%. The reason why penalty costs occupy a place is the instability of hydrogen generation from renewable energy, which causes hydrogen shortage or abandonment when hydrogen is supplied. Under the 10 MW PV design condition,

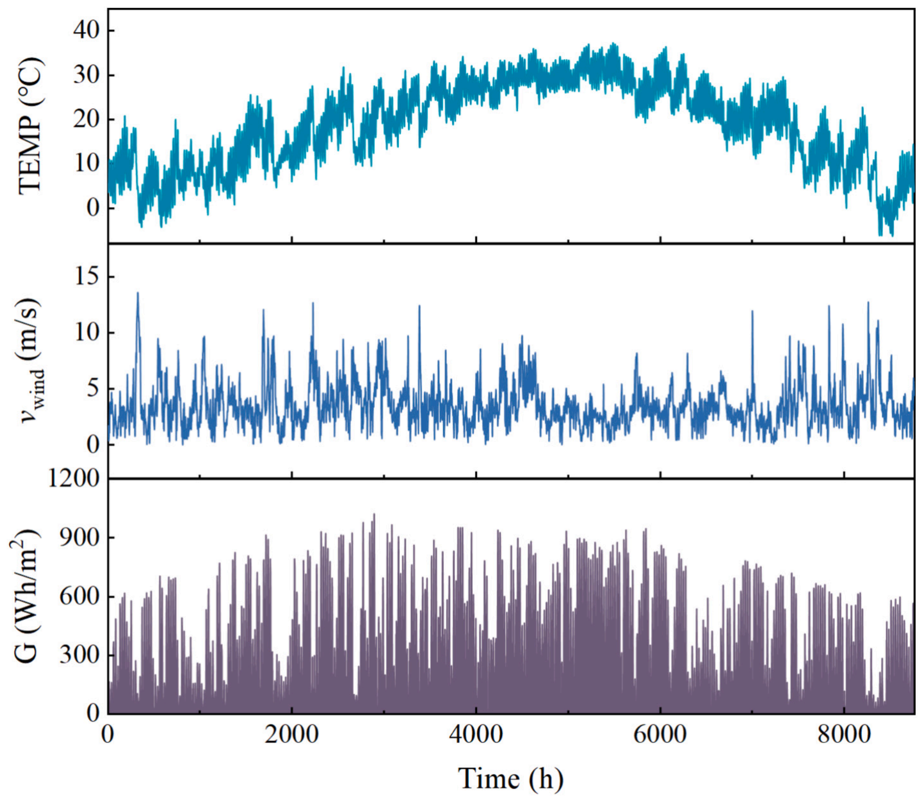

Fig. 9. Annual hourly weather conditions in Wuhan.

Table 4
Decision variable boundaries.

Parameter	Lower boundary	Higher boundary
PEME electrolyzer capacity, $P_{ELK,\ R}$ (MW)	3	10
Battery capacity, $E_{batt,\ R}$ (MWh)	1	3
H2 tank capacity, $M_{H2,\ tank,\ R}$ (kg)	500	3000
Renewable energy penetration rate, (%)	70	–

Table 5
Electricity prices at different times.

Item	Value (RMB/kWh)
Peak power (8:00–11:00, 18:00–22:00)	0.974
Valley electricity (23:00–7:00)	0.318
Flat electricity (others)	0.629

Table 6
Key economic parameters [45,46].

Item	Investment (RMB/kW)	Replacement (RMB/kW)	O&M (RMB/(kW·year))	Lifetime (year)
PV plant	4130	1945	50	25
Wind farm	5785	2000	60	20
Electrolyzer	10,000	5000	200	20
Battery	1629	1075	81	5
Hydrogen tank	2960	2960	148	20
Inverter	272	272	12	10
Transformer	200	200	10	10

$LCOH_{PV}$ is 11.62 RMB/kg (or USD 1.63 per kg), which is less than the electrolyzer cost of 14.63 RMB/kg (or USD 2.05 per kg), while the power cost under the other two conditions is higher than $LCOH_{ELK}$. This is because LCOE under the three power generation methods is different, 10 MW PV is 0.2243 RMB/kWh (or USD 31.10 per MWh), higher than 0.1824 RMB/kWh (USD 25.54 per MWh) and 0.1979 RMB/kWh (or USD 27.71 perMWh). In Fig. 11(b), the largest proportion of the LCOH of the grid-connected system is the cost of electricity and electrolyzer. Compared with off-grid, grid-connected systems can purchase and sell electricity from the grid, and the penalty costs caused by power abandonment and unstable hydrogen supply are greatly reduced. Whether off-grid or grid-connected, wind power hydrogen generation is cheaper than PV, but PV has an approximately periodic fluctuation, and wind power has a large unpredictability, which will lead to an increase in the start and stop frequency of the electrolyzer and reduce the service life of the equipment. Although the cost of grid-connected hydrogen generation is lower than that of off-grid, the power generation capacity of WT and PV is highly correlated with natural conditions (such as wind speed and sunshine intensity), and there is significant volatility and randomness. The fluctuation of grid frequency and voltage exceeds the allowable range, which may damage power equipment and user equipment.

Table 8 presents a comparison of previous literature on the economics of hydrogen production under comparable system boundaries, including PV-PEM, wind-PEM, and hybrid PV-wind-PEM systems. The comparison covers key assumptions such as electricity cost, PEM electrolyzer stack lifetime, hydrogen compression and storage pressure, as well as whether BoP and water treatment are included or excluded. Overall, Table 8 shows significant variation in LCOH reported in recent literature (approximately 1.62–12.38 USD/kg), reflecting the sensitivity of research outcomes to technological cost assumptions and boundary definitions. In this study, LCOH values ranging from 2.89 to 4.92 USD/kg fall within the scope of comparable photovoltaic/wind-driven PEM studies. Differences across literature are often attributable to variations in renewable energy unit costs (e.g., capital expenditures for PV and wind), electrolyzer stack replacement assumptions (e.g., lifespan expressed in years or operating hours), and downstream requirements (e.g., target compression/storage conditions). It is important to note that several studies differ in whether they include BoP equipment and water

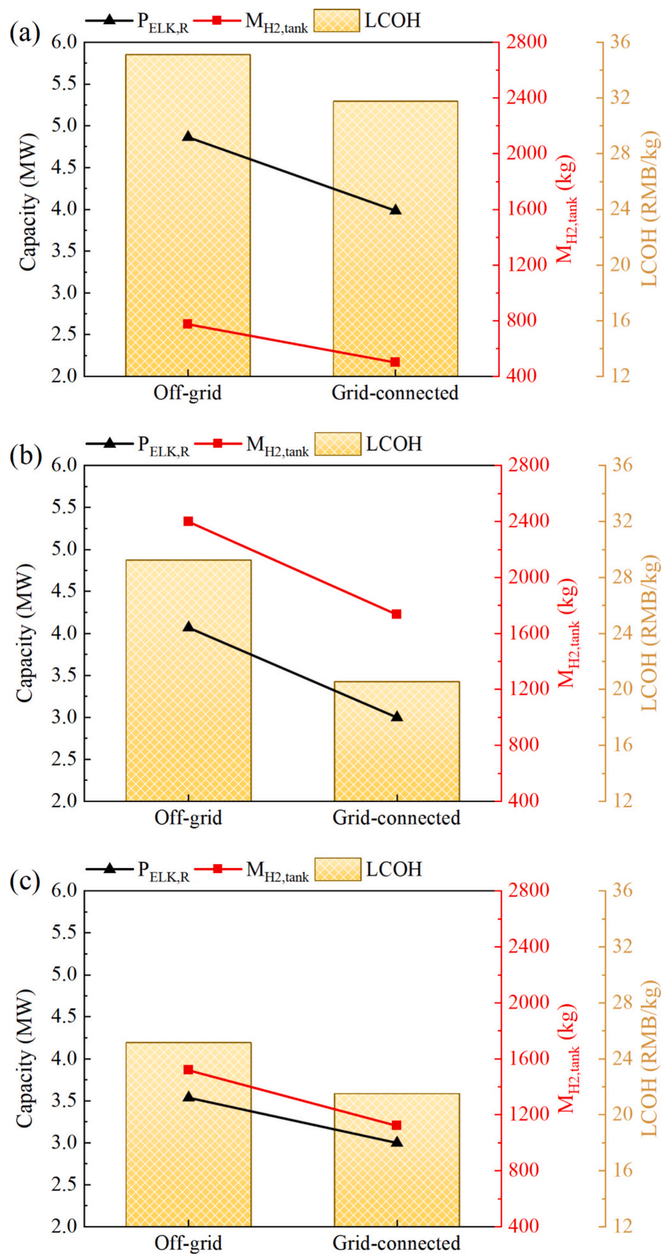

Fig. 10. Optimal sizing and LCOH of systems: (a)10 MW PV, (b)10 MW WT, (c) 5 MW PV + 5 MW WT.

treatment processes. Therefore, this comparison is presented primarily as a scenario benchmark reference rather than a strict ranking. Readers are advised to interpret the competitiveness assessment results in conjunction with the listed assumptions and boundary selections.

3.5. Uncertainty analysis

Intermittent operating modes may impact the lifespan of PEM stacks, particularly under start-stop or load cycling conditions. Although the model employs fixed component lifetimes and replacement cycles, these operational factors can influence the stack degradation rate, thereby affecting its performance. Therefore, this study conducted a sensitivity analysis on the stack replacement interval affecting LCOH, focusing on the number of stack replacements (Nrepl). Fig. 12 shows the sensitivity case on stack replacement interval for PV and WT in off-grid scenarios. Under ideal conditions, with no stack replacement, LCOH is 35.11 RMB/kg and 29.25 RMB/kg (or USD 4.92 and USD 4.10 per kg). When the stack is replaced 1–2 times, LCOH is 36.64 RMB/kg-40.20 RMB/kg (or USD 5.13–5.63 per kg) and 30.16 RMB/kg-32.27 RMB/kg (or USD 4.22–4.52 per kg). Under a more conservative estimate, with a stack replacement interval of 4 years to 6 years, replacing the stack 3–4 times results in LCOH of 42.93 RMB/kg-47.13 RMB/kg (or USD 6.01–6.60 per kg) and 33.88 RMB/kg-36.38 RMB/kg (or USD 4.74–5.09 per kg).

Sensitivity analysis (SI section B) results indicate that LCOH is significantly influenced by the costs of renewable energy components and electrolysis equipment. In actual production, the LCOE determined by renewable energy generation component costs and grid electricity prices exhibit certain fluctuations. Therefore, it is necessary to conduct uncertainty analysis to identify key uncertainty factors and quantify their impact on system output. This facilitates more robust decision-making, enabling the prediction of possible ranges of system behavior through scenario simulations even under data-scarce conditions. Performing uncertainty analysis using the Monte Carlo simulation method. In the absence of sufficiently robust joint statistics to parameterize cross-correlations, the benchmark Monte Carlo implementation treats uncertain inputs as independent variables. We explicitly note that the presence of correlations may alter the tail distribution characteristics of LCOH results, identifying this as a limitation of the current methodology. We further indicate that addressing this will be a future direction for improvement when joint datasets become available. To enhance transparency regarding random input parameters, we compiled the mean, standard deviation, sample size, empirical probability density distribution formed by Monte Carlo samples, R^2 and RMSE between this distribution and the theoretical normal probability density function for renewable electricity costs, grid electricity prices, and electrolyzer capital expenditures. Corresponding data sources are also annotated, as shown in Table 9. Fig. 13 displays the normal probability density distributions and Monte Carlo sample points for renewable electricity prices (LCOE), grid electricity prices, and electrolyzer CAPEX. This allows for an intuitive visualization of the distribution and range of uncertainty associated with the hypothesis. Simultaneously, truncated normal distributions are applied to grid electricity prices and electrolyzer CAPEX to prevent non-physical values.

The Table 9 reports the Monte Carlo sampling scale, while Fig. 14 and Fig. 15 provides an empirical mapping between quantiles and results. In the finite sample results, the proportion of outcomes below the P90 threshold exceeds 0.93 (28/30) due to discrete sampling, indicating that estimates of upper tail cost levels are stable. The cumulative probability (CP) curves of LCOH affected by electricity price fluctuations under different scenarios are shown in Fig. 14. For LCOE fluctuations

Table 7
Key assumptions, optimized dimensions, and grid interaction under different configurations.

Configuration	PV (MW)	WT (MW)	Electrolyzer (MW)	number of modules	Electricity Purchase (MWh/year)	Electricity sold (MWh/year)
Off-grid PV	10	0	4.86	195	0	0
Off-grid WT	0	10	4.07	163	0	0
Off-grid PV + WT	5	5	3.54	142	0	0
Grid-connected PV	10	0	3.98	160	3301.75	900.60
Grid-connected WT	0	10	3.00	120	2741.46	5159.01
Grid-connected PV + WT	5	5	3.00	120	1855.54	1765.31

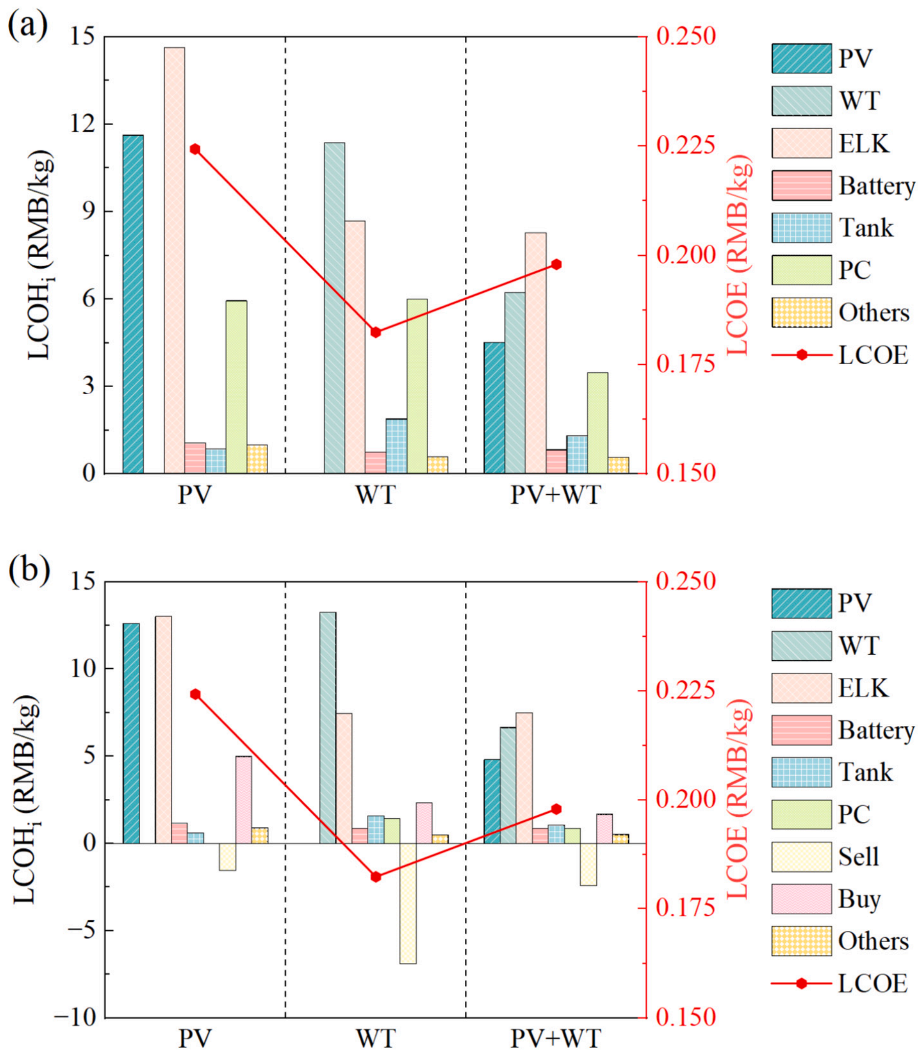

Fig. 11. Cost composition and LCOE of off-grid and grid-connected systems: (a) off-grid, (b) grid-connected.

Table 8
Comparison of previous literature about economics of hydrogen production.

Author(s)	LCOH (USD/kg)	PV unit cost (USD/kW)	Wind unit cost (USD/kW)	Stack lifetime	Compression & storage pressure	BoP and water treatment	[Ref.]
This study	2.89–4.92	578	810	20 years	2 MPa	Inclusion	This study
Berrada, A. et al. (2023).	2.53–3.62	340	3440	60,000 h	Compressor capacity 5100 kg/h	Inclusion	[47]
Zheng, Y. et al. (2023).	4.30–5.00	N/A	1547	15 years	–	–	[30]
Fabianek, P., & Madlener, R. (2024).	4.50–5.30	1301	1483	–	–	Inclusion	[48]
Hill, P. et al. (2024).	9.89–12.38	N/A	1652	7 years	–	Inclusion	[49]
Arias, I. et al. (2024).	1.62–3.30	610	N/A	90,000 h	8 MPa	Inclusion	[50]

(standard deviation 0.0212 RMB/kWh or USD 2.97 per MWh): Off-grid, a unit hydrogen production at a cumulative probability value of 0.5 is 34.84 RMB/kg, 31.57 RMB/kg, 29.74 RMB/kg (or USD 4.88, 4.42, 4.16 per kg), PV + WT exhibits the broadest cumulative probability curve (5.80 RMB/kg or USD 0.81 per kg), while PV has the narrowest (4.31 RMB/kg or USD 0.81 per kg); On-grid, a unit hydrogen production at a cumulative probability value of 0.5 is 27.71 RMB/kg, 19.50 RMB/kg, 20.42 RMB/kg (USD 3.88, 2.73, 2.86 per kg). WT exhibits the widest range (4.63 RMB/kg or USD 0.65 per kg), while PV has the narrowest (3.26 RMB/kg or USD 0.46 per kg). For grid electricity price fluctuations (standard deviation 0.3281 RMB/kWh or USD 45.93 per MWh): Under grid connection, hydrogen production at a cumulative probability value of 0.5 is 35.98 RMB/kg, 19.85 RMB/kg, and 21.73 RMB/kg (USD 5.04, 2.78 per kg), with WT exhibiting the widest range (13.19 RMB/kg or USD 1.85 per kg), while PV + WT exhibits the narrowest range (1.26 RMB/kg or USD 0.18 per kg). This correlation relates to the stability of renewable electricity supply.

In addition to electricity cost uncertainty, electrolyzer CAPEX were also incorporated as an uncertainty driver in the Monte Carlo analysis due to the significant impact observed in the sensitivity study. The cumulative probability of LCOH affected by electrolyzer capital expenditure uncertainty is shown in Fig. 15. Off-grid (Fig. 15(a)), PV + WT

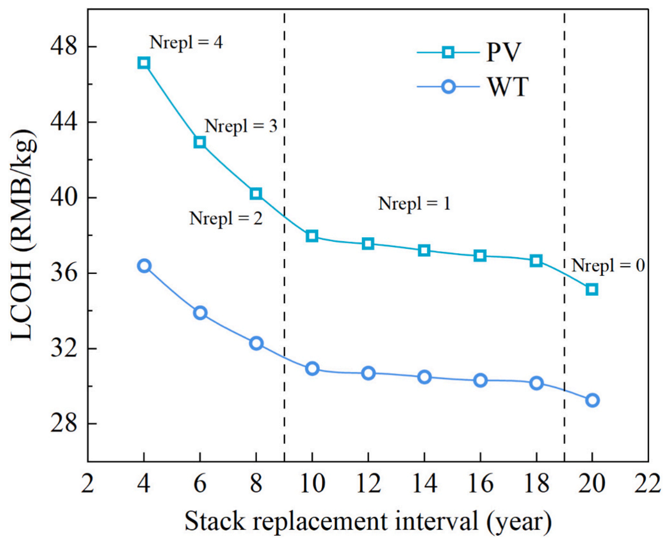

Fig. 12. The sensitivity case on stack replacement interval for PV and WT in off-grid scenarios.

achieves the lowest LCOH, with LCOH PV + WT at CP = 0.5 estimated around 30.99 RMB/kg or USD 4.34 per kg. For grid-connected scenarios (Fig. 15(b)), the WT power supply configuration proves economically optimal (CP = 0.5, LCOH ~21.88 RMB/kg or USD 3.06 per kg). This is because ample power availability and grid stability enhancement in this mode allow for lower required electrolyzer capacity compared to other options. In the PV scenario, due to higher electrolyzer capacity requirements, LCOH uncertainty ranges are wider at CP = 0.9, fluctuating between 27.31 and 50.31 RMB/kg (or USD 3.82–7.04 per kg) and 24.53–44.06 RMB/kg (or USD 3.43–6.17 per kg). Compared to electricity costs, the uncertainty in electrolyzer CAPEX has a more significant impact on LCOH.

4. Discussion

The findings of this study prove that modular PEME systems offer potential advantages compared with centralized hydrogen production infrastructure in terms of investment and deployment flexibility. The modular architecture enables phased investment on integrable units, which enables more efficient matching with renewable energy fluctuations. The wide deployment of MHS can lead to substantial reductions in CAPEX through multiple avenues, including reduced land use and lowered site construction and development costs. For example, the 25-kW modular PEME system presented in this study can save RMB 2.62 million (or USD 366.80) in CAPEX, demonstrating the inherent economic advantage of distributed deployment in upfront investment. Furthermore, the mobility of modular systems allows flexible redeployment between different wind and solar resource zones via truck transport, partially alleviating the spatiotemporal mismatch of energy resources and enhancing renewable energy utilization efficiency. However, the modular architecture also introduces additional economic burdens, such as transportation costs incurred during system relocation and on-site integration. The cumulative effect of these costs becomes more pronounced with increased transportation frequency. This study found that under the assumption of relocating five times over a 20-year lifetime, transportation costs could reach up to RMB 1.12 million (or USD 156.80). Nevertheless, comprehensive LCOH analysis indicates that even when accounting for transportation expenses, modular systems maintain a competitive advantage in hydrogen production costs across most application scenarios, demonstrating their overall economic viability.

Compared to existing literature, the primary contribution of this study lies in providing a comprehensive system-level analysis framework that integrates system designs with engineering and economic models, which also encompasses system costs, transportation impacts, renewable energy adaptability, and uncertainty assessment. Previous research has primarily focused on multi-stack cooperative operation, energy allocation optimization, or system control strategies, lacking a holistic quantitative evaluation of the economic viability, risk profile, and system adaptability of modular architectures across different deployment scenarios [55–58]. This study systematically examines, for the first time, how modular PEME systems reduce CAPEX, enhance capacity utilization, and perform economically in fluctuating wind and solar environments. It further analyzes whether the transportation costs introduced by modular characteristics offset their economic advantages. Additionally, this study constructs a PSO-Monte Carlo hybrid optimization framework that incorporates uncertainty propagation and cost-driver sensitivity analysis, addressing the current literature gap in risk perception for modular PEME systems. Consequently, this research establishes the first quantitative strategy evaluation system for modular PEME systems in renewable energy coupling scenarios, providing system designers and decision-makers with a more comprehensive techno-economic support.

Although this study provides a systematic economic and adaptability analysis, several limitations remain. The CAPEX savings reported in this study (e.g., RMB 2.62 million or USD 366.80k) are scenario-based estimates derived under China-specific land-use and construction cost assumptions; therefore, they should be interpreted as indicative results within the Chinese context rather than universally transferable values. First, the modeling is based on a 25-kW demonstration scale, failing to capture the synergistic optimization effects of larger modular clusters (e.g., 100 kW–MW scale), whose performance and economics may exhibit nonlinear changes at scaled-up levels. Second, the transportation cost model may over assume fixed routes and frequencies, whereas real-world scheduling may be influenced by seasonal variations, road conditions, regional policies, and other factors. Third, the techno-economic model does not incorporate long-term dynamic factors such as stack aging, optimized O&M strategies, or climate-induced system performance variations. The critical trade-offs involving efficiency, utilization, performance degradation, and operational flexibility have not been explored through a multi-objective optimization model. In addition, the power consumption of auxiliary equipment may impact the overall energy efficiency of the system. Future work may explore the following

Table 9
Basis for uncertainty setting.

Item	Sources	Mean	Standard deviation	Sample size	R2	RMSE
LCOE	Calculated based on Wuhan meteorological data from 2020 to 2024 [51]	0.2039 RMB/kWh (USD 28.55 per MWh)	0.0212 RMB/kWh (USD 2.97 per MWh)	30	0.9739	0.1520
Grid electricity prices	Electricity prices by the hour in China [43]	0.6417 RMB/kWh (USD 89.84 per MWh)	0.3281 RMB/kWh (USD 45.93 per MWh)	30	0.8523	1.0451
Electrolyzer CAPEX	[30,47–50,52–54]	11,419 RMB (USD 1569)	4826 RMB (USD 676)	30	0.9651	5.1253×10^{-6}

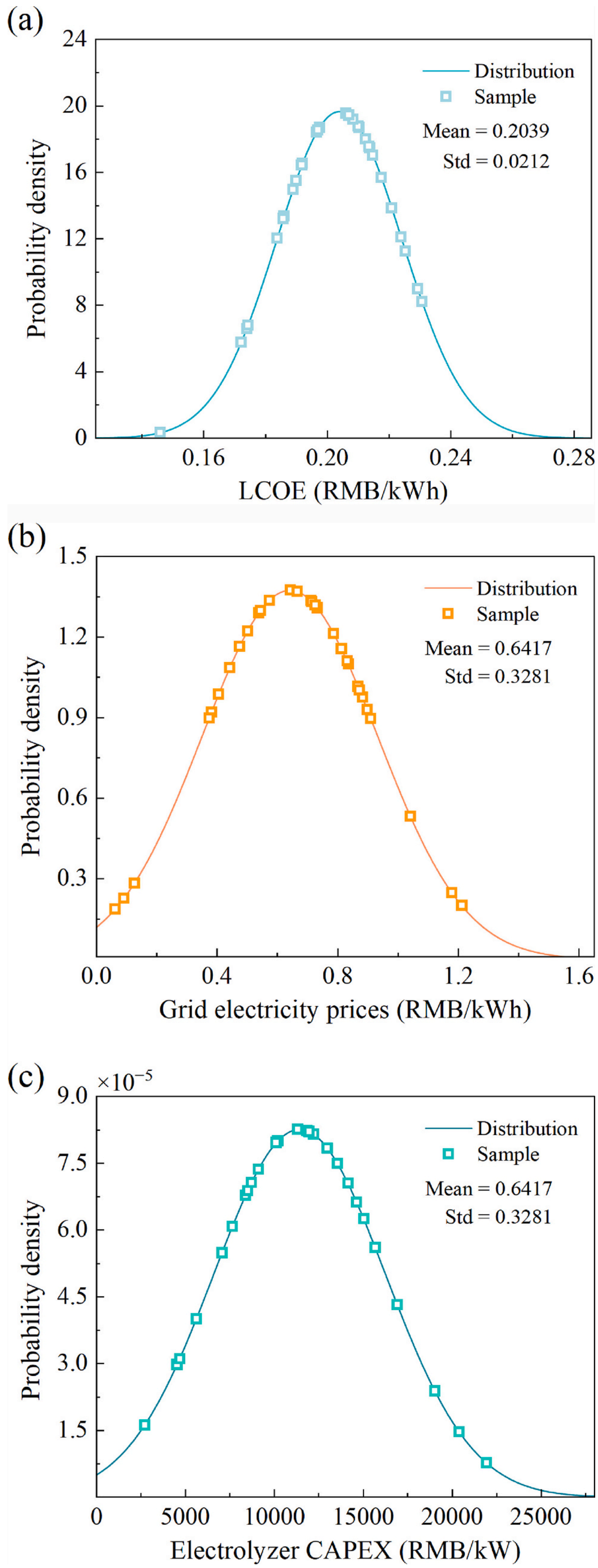

Fig. 13. Normal probability density distribution and Monte Carlo sample points: (a) renewable electricity prices (LCOE), (b) grid electricity prices, (c) electrolyzer CAPEX.

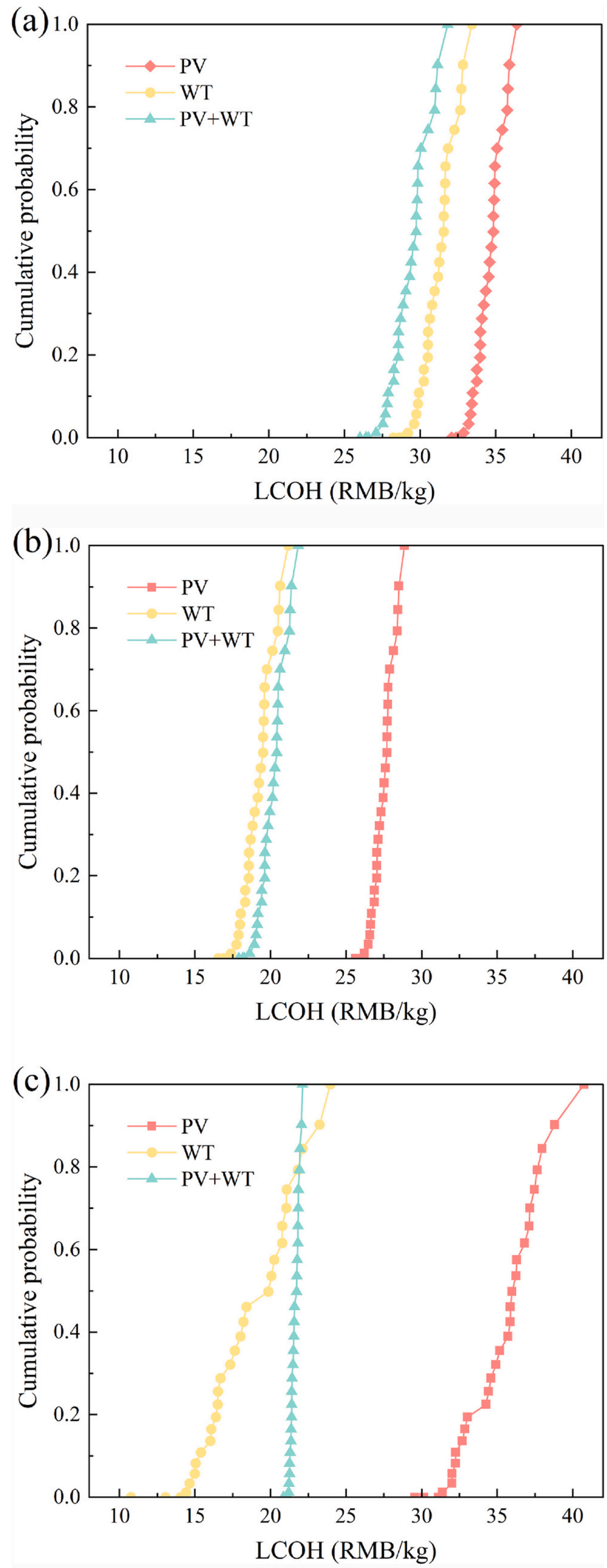

Fig. 14. Cumulative probability of LCOH across different key factors: (a) uncertainty of LCOE on off-grid, (b) uncertainty of LCOE on grid-connected, (c) uncertainty of grid electricity prices on grid-connected.

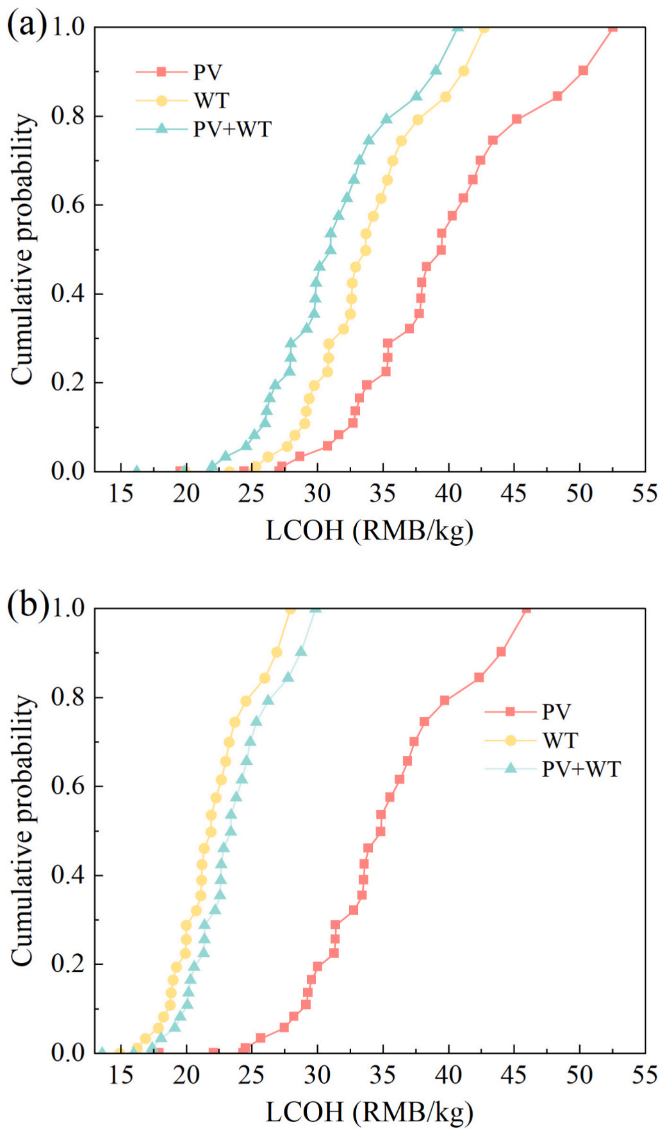

Fig. 15. Cumulative probability of LCOH across electrolyzer CAPEX: (a) off-grid, (b) grid-connected.

directions: (1) Develop a cross-regional, multi-node modular hydrogen production scheduling model to optimize regional hydrogen production capacity allocation; (2) Incorporate stack degradation behavior into full life-cycle simulations to investigate the impact of modular architecture on lifetime costs, and integrate system energy efficiency into optimization metrics to explore trade-offs among multiple objectives; (3) Conduct longer-term temporal optimization using real-time wind and solar resource data; (4) Emerging modular systems with hydrogen storage and transportation to construct a more comprehensive economic model for the hydrogen value chains; (5) Further explore the impact of these auxiliary powers on the overall system performance and consider incorporating them into a more comprehensive energy efficiency assessment.

Importantly, China possesses one of the world's most abundant renewable energy resources, particularly in remote regions such as Xinjiang, Qinghai, Tibet, and Gansu, where wind and solar energy potential accounts for approximately 40–50% of the national total [59–61]. However, these areas often feature vast expanses of land with sparse populations and limited infrastructure, making it challenging to construct centralized, fixed-site large-scale hydrogen production plants. This hinders the local consumption of renewable energy resources. The mobile modular PEME system proposed in this study offers flexible hydrogen production in regions abundant in wind and solar resources but lacking supporting energy infrastructure, filling the application gap left by centralized hydrogen production. By producing hydrogen locally at the resource source and dynamically relocating modules based on demand, it significantly enhances renewable energy utilization while reducing energy losses from long-distance transmission or curtailed wind and solar power. More importantly, the system's low CAPEX and low LCOH make it a deployable solution for green hydrogen production in developing regions, small-to-medium industrial parks, and remote settings. This research holds significant implications for advancing distributed green hydrogen infrastructure development in China and globally, potentially accelerating the large-scale application of hydrogen energy in the energy transition.

5. Conclusions

This study presented a modular PEME hydrogen production system, showcasing the advantages of CAPEX savings, enhancing renewable resource conversion efficiency and transportation impacts. We investigated the capacity configuration of the energy system for six scenarios involving PV, WT and hybrid electricity supply. The LCOH for the renewable energy-coupled PEME electrolysis hydrogen production system under the optimized configuration was analyzed. Sensitivity analysis of system hydrogen production costs and analysis of electricity price uncertainty analysis were conducted using Monte-Carlo simulation. The main conclusions are articulated as follows:

(1) The proposed 25-kW modular PEME system reduces land use by 5760 square meters and saves approximately RMB 0.52 million (or USD 72.80k) in CAPEX, decreases electrolyzer construction investment by RMB 1.62 million (or USD 226.80k) and equipment installation costs by RMB 0.48 million (or USD 67.20k), resulting in total capital expenditure savings of approximately RMB 2.62 million (or USD 366.80k).
(2) Assuming a 20-year lifespan and a capacity of 6 MW. System relocation incurs additional transportation costs of up to RMB 1.12 million (or USD 156.80k).
(3) It exhibits a lower levelized cost of hydrogen (LCOH) under grid-connected and wind power design conditions. Under the off-grid scheme, the most economical hydrogen generation from PV-WT power generation is 25.17 RMB/kg (or USD 3.52 per kg); under the grid-connected scheme, the LCOH of hydrogen generation from WT power generation is the lowest, at 20.55 RMB/kg (or USD 2.88 per kg). Power generation equipment and electrolysis device costs constitute the primary contributors to system expenses.
(4) The LCOH of the renewable energy hydrogen generation system is sensitive to the cost of WT, PV modules, and PEME electrolyzer. For LCOE fluctuations: Off-grid, PV + WT exhibits the broadest cumulative probability curve while PV has the narrowest; On-grid, WT exhibits the widest range, while PV has the narrowest. For grid electricity price fluctuations: Under grid connection, with WT exhibiting the widest range, while PV + WT exhibits the narrowest range. This correlation relates to the stability of renewable electricity supply.

Declaration of using generative AI

The authors declare using ChatGPT to assist with language editing and refinement of the manuscript. The tool did not generate or modify the scientific concepts, methods, data, results, or conclusions presented herein. All intellectual content is original to the authors, and all AI-assisted text was carefully reviewed, validated, and edited by the authors to ensure accuracy and compliance with journal standards.

CRediT authorship contribution statement

Jie Yang: Writing – review & editing, Writing – original draft, Visualization, Validation, Software, Methodology, Investigation, Formal analysis, Data curation. **Jichong Yang:** Visualization, Validation, Supervision, Resources, Methodology, Investigation. **Ke Chang:** Validation, Supervision, Software, Resources, Investigation. **Chengcheng Lyu:** Writing – review & editing. **Haoming Ma:** Writing – review & editing. **Qiang Cheng:** Resources, Project administration, Methodology, Funding acquisition, Formal analysis, Conceptualization. **Zixue Luo:** Writing – review & editing, Supervision, Resources, Methodology, Funding acquisition, Formal analysis, Conceptualization.

Declaration of competing interest

The authors declare that they have no known competing financial interests or personal relationships that could have appeared to influence the work reported in this paper.

Acknowledgment

This work was supported by the National Key Research and Development Program of China (No. 2024YFB4007100), with support to J. Y., J. Y., and Q. C.

Appendix A. Methods, Sensitivity Analysis, and Supporting Data

Supplementary data to this article can be found online at https://doi.org/10.1016/j.apenergy.2026.127759.

Data availability

The data supporting the findings of this study are available within the Supplementary Information. Additional datasets or model outputs used in this analysis can be made available from the corresponding author upon reasonable request.

References

[1] Herdem MS, Mazzeo D, Matera N, Baglivo C, Khan N, Afnan, et al. A brief overview of solar and wind-based green hydrogen production systems: trends and standardization. Int J Hydrog Energy 2024;51:340–53. https://doi.org/10.1016/j.ijhydene.2023.05.172.
[2] Jiang Y, Huang W, Yang G. Electrolysis plant size optimization and benefit analysis of a far offshore wind-hydrogen system based on information gap decision theory and chance constraints programming. Int J Hydrog Energy 2022;47:5720–32. https://doi.org/10.1016/j.ijhydene.2021.11.211.
[3] Brahim T, Jemni A. Green hydrogen production: a review of technologies, challenges, and hybrid system optimization. Renew Sust Energ Rev 2026;225:116194. https://doi.org/10.1016/j.rser.2025.116194.
[4] Algburi S, Munther H, Al-Dulaimi O, Fakhruldeen HF, Sapaev IB, Seedi KFKA, et al. Green hydrogen role in sustainable energy transformations: a review. Results Eng 2025;26:105109. https://doi.org/10.1016/j.rineng.2025.105109.
[5] IEA. Global Hydrogen Review 2025. 2025. p. https://www.iea.org/reports/global-hydrogen-review-2025.
[6] IEA. World Energy Outlook 2025. 2025. p. https://www.iea.org/reports/world-energy-outlook-2025.
[7] Singla MK, Gupta J, Beryozkina S, Safaraliev M, Singh M. The colorful economics of hydrogen: assessing the costs and viability of different hydrogen production methods - a review. Int J Hydrog Energy 2024;61:664–77. https://doi.org/10.1016/j.ijhydene.2024.02.255.
[8] Fan J, Yu P, Li K, Xu M, Zhang X. A levelized cost of hydrogen (LCOH) comparison of coal-to-hydrogen with CCS and water electrolysis powered by renewable energy in China. Energy (Oxford) 2022;242:123003. https://doi.org/10.1016/j.energy.2021.123003.
[9] Ordóñez DF, Ganzer C, Halfdanarson T, Garay AG, Patrizio P, Bardow A, et al. Quantifying global costs of reliable green hydrogen. Energy Adv 2023;2:2042–54. https://doi.org/10.1039/d3ya00318c.
[10] Wen Q, Liu G, Rao Z, Liao S. Applications, evaluations and supportive strategies of distributed energy systems: a review. Energ Buildings 2020;225:110314. https://doi.org/10.1016/j.enbuild.2020.110314.
[11] Yue M, Lambert H, Pahon E, Roche R, Jemei S, Hissel D. Hydrogen energy systems: a critical review of technologies, applications, trends and challenges. Renew Sust Energ Rev 2021;146:111180. https://doi.org/10.1016/j.rser.2021.111180.
[12] Hanley ES, Deane JP, Gallachóir BÓ. The role of hydrogen in low carbon energy futures–a review of existing perspectives. Renew Sust Energ Rev 2018;82:3027–45. https://doi.org/10.1016/j.rser.2017.10.034.
[13] Fonseca JD, Camargo M, Commenge J, Falk L, Gil ID. Trends in design of distributed energy systems using hydrogen as energy vector: a systematic literature review. Int J Hydrog Energy 2019;44:9486–504. https://doi.org/10.1016/j.ijhydene.2018.09.177.
[14] Carmo M, Fritz DL, Mergel J, Stolten D. A comprehensive review on PEM water electrolysis. Int J Hydrog Energy 2013;38:4901–34. https://doi.org/10.1016/j.ijhydene.2013.01.151.
[15] Buttler A, Spliethoff H. Current status of water electrolysis for energy storage, grid balancing and sector coupling via power-to-gas and power-to-liquids: a review. Renew Sust Energ Rev 2018;82:2440–54. https://doi.org/10.1016/j.rser.2017.09.003.
[16] Wirkert FJ, Roth J, Jagalski S, Neuhaus P, Rost U, Brodmann M. A modular design approach for PEM electrolyser systems with homogeneous operation conditions and highly efficient heat management. Int J Hydrog Energy 2020;45:1226–35. https://doi.org/10.1016/j.ijhydene.2019.03.185.
[17] Nnabuife SG, Hamzat AK, Whidborne J, Kuang B, Jenkins KW. Integration of renewable energy sources in tandem with electrolysis: a technology review for green hydrogen production. Int J Hydrog Energy 2024. https://doi.org/10.1016/j.ijhydene.2024.06.342.
[18] El-Hamalawy AF, Farag HEZ, Asif A. Multi-objective optimal modular design of PEM electrolyzers for efficient and scalable green hydrogen production plants. J Power Sources 2025;637:236510. https://doi.org/10.1016/j.jpowsour.2025.236510.
[19] Cooper N, Horend C, Röben F, Bardow A, Shah N. A framework for the design & operation of a large-scale wind-powered hydrogen electrolyzer hub. Int J Hydrog Energy 2022;47:8671–86. https://doi.org/10.1016/j.ijhydene.2021.12.225.
[20] Zhu P, Mae M, Matsuhashi R. Techno-economic analysis of grid-connected hydrogen production via water electrolysis. Energies (Basel) 2024;17:1653. https://doi.org/10.3390/en17071653.
[21] Aminaho EN, Aminaho NS, Aminaho F. Techno-economic assessments of electrolyzers for hydrogen production. Appl Energy 2025;399:126515. https://doi.org/10.1016/j.apenergy.2025.126515.
[22] Markaj A, Lorenz J, Scholz L, Henkel V, Fay A. Towards a systematic and knowledge-based requirements and conceptual engineering for modular electrolysis plants. Energy. Inform 2023:6. https://doi.org/10.1186/s42162-023-00298-9.
[23] Makhsoos A, Kandidayeni M, Ziane MA, Moghadari M, Boulon L, Pollet BG. Energy management for modular proton exchange membrane water electrolyzers under fluctuating solar inputs: a constrained nonlinear optimization approach. Appl Energy 2025;394:126124. https://doi.org/10.1016/j.apenergy.2025.126124.
[24] Makhsoos A, Kandidayeni M, Ziane MA, Boulon L, Pollet BG. Model benchmarking for PEM water Electrolyzer for energy management purposes. Energy Convers Manag 2025;323:119203. https://doi.org/10.1016/j.enconman.2024.119203.
[25] Eikeng E, Makhsoos A, Pollet BG. Critical and strategic raw materials for electrolysers, fuel cells, metal hydrides and hydrogen separation technologies. Int J Hydrog Energy 2024;71:433–64. https://doi.org/10.1016/j.ijhydene.2024.05.096.
[26] Makhsoos A, Kandidayeni M, Boulon L, Pollet BG. A comparative analysis of single and modular proton exchange membrane water electrolyzers for green hydrogen production- a case study in Trois-Rivières. Energy (Oxford) 2023;282:128911. https://doi.org/10.1016/j.energy.2023.128911.
[27] Köstlbacher J, Breuning L, Nigbur F, Wienert P, Khatiwada D. Application of an electrolysis system model for techno-economic optimization of hydrogen production in industry-based case studies. Int J Hydrog Energy 2025;138:1144–62. https://doi.org/10.1016/j.ijhydene.2025.03.291.
[28] Wang X, Meng X, Nie G, Li B, Yang H, He M. Optimization of hydrogen production in multi-Electrolyzer systems: a novel control strategy for enhanced renewable energy utilization and Electrolyzer lifespan. Appl Energy 2024;376:124299. https://doi.org/10.1016/j.apenergy.2024.124299.
[29] Gao X, Wang X, Zheng L, Zhang S, Zhang X. Techno-economic optimization of a coupled electricity-heat-hydrogen energy system considering seasonal hydrogen storage and demand response. Int J Hydrog Energy 2025;180:151642. https://doi.org/10.1016/j.ijhydene.2025.151642.
[30] Zheng Y, Huang C, Tan J, You S, Zong Y, Træholt C. Off-grid wind/hydrogen systems with multi-electrolyzers: optimized operational strategies. Energy Convers Manag 2023;295:117622. https://doi.org/10.1016/j.enconman.2023.117622.
[31] Henkel V, Wagner LP, Kilthau M, Gehlhoff F, Fay A. A multi-agent approach for the optimized operation of modular electrolysis plants. Energies (Basel) 2024;17:3370. https://doi.org/10.3390/en17143370.
[32] Evro S, Tomomewo OS. Green hydrogen integration in distributed energy systems: a comprehensive techno-economic and policy analysis. Int J Hydrog Energy 2025;148:149895. https://doi.org/10.1016/j.ijhydene.2025.06.085.
[33] Schofield L, Paren B, Macdonald R, Horn YS, Mallapragada D. Dynamic optimization of proton exchange membrane water electrolyzers considering usage-based degradation. AICHE J 2024:71. https://doi.org/10.1002/aic.18635.
[34] Zhang H, Yuan T. Optimization and economic evaluation of a PEM electrolysis system considering its degradation in variable-power operations. Appl Energy 2022;324:119760. https://doi.org/10.1016/j.apenergy.2022.119760.
[35] Zheng W, Lv B, Shao Z, Zhang B, Liu Z, Sun J, et al. Optimization of power allocation for the multi-stack PEMEC system considering energy efficiency and degradation. Int J Hydrog Energy 2024;53:1210–25. https://doi.org/10.1016/j.ijhydene.2023.11.241.
[36] Guo F, Li Y, Shi H, Qu J, Tan W. Optimization of power distribution for multi-stack electrolyzers system considering hydrogen production and voltage degradation. Int

J Hydrog Energy 2025;175:151452. https://doi.org/10.1016/j.ijhydene.2025.151452.
[37] He Y, Guo S, Zhou J, Wu F, Huang J, Pei H. The quantitative techno-economic comparisons and multi-objective capacity optimization of wind-photovoltaic hybrid power system considering different energy storage technologies. Energy Convers Manag 2021;229:113779. https://doi.org/10.1016/j.enconman.2020.113779.
[38] Tang O, Rehme J, Cerin P. Levelized cost of hydrogen for refueling stations with solar PV and wind in Sweden: on-grid or off-grid? Energy (Oxford) 2022;241:122906. https://doi.org/10.1016/j.energy.2021.122906.
[39] Tebibel H. Methodology for multi-objective optimization of wind turbine/battery / electrolyzer system for decentralized clean hydrogen production using an adapted power management strategy for low wind speed conditions. Energy Convers Manag 2021;238:23. https://doi.org/10.1016/j.enconman.2021.114125.
[40] Shanghai Environment and Energy Exchange. https://www.cneeex.com/dtfw/lsjr/lszq/zgqjzs/zgqjzstxjgfb/.
[41] Yang J, Chi H, Cheng M, Dong M, Li S, Yao H. Performance analysis of hydrogen supply using curtailed power from a solar-wind-storage power system. Renew Energy 2023;212:1005–19. https://doi.org/10.1016/j.renene.2023.05.094.
[42] Xu J, Ding X, Gong Y, He G, Hu T. Economic analysis of hydrogen production plant with water electrolysis. Energy Storage Sci Technol 2022;11:2374–85. https://doi.org/10.19799/j.cnki.2095-4239.2022.0062.
[43] Sun X, Cheng X, Wang S, Wang J, Zhao Y, Zhang B. Dynamic cost analysis of hydrogen production from wind power and photovoltaic power. Clean Coal Technol 2023;29:1–10. https://doi.org/10.13226/j.issn.1006-6772.CN22071501.
[44] Terlouw T, Bauer C, McKenna R, Mazzotti M. Large-scale hydrogen production via water electrolysis: a techno-economic and environmental assessment. Energy Environ Sci 2022;15:3583–602. https://doi.org/10.1039/d2ee01023b.
[45] Liu Q. Simulation study of hydrogen production system for wind and solar power generation coupled with PEM water electrolysis [M]. Huazhong University of Science and Technology 2024. https://kns.cnki.net/kcms2/article/abstract?v=LYi8dJWcB0V1kuN4YIIOsDjSNfPeu2p_janmAKiSph6Ht3JAqb4pJQGT-2-yIeor-s10KVFEtOq_IQY9UgR8c2CXhYMjgHWSvKx967tzqAmnvBtNsGnDIrMeGhTlXBgqJcsPdPq2g7E0o3LF_NjM8ZMJ647mOA5V01HA7gAtsQk=&uniplatformDoi: 10.27157/d.cnki.ghzku.2024.004603.
[46] Wen C, Zhang B, Wang Y, Liu Q, Tu Z, Zhang Z, et al. Research progress of high efficiency proton exchange membrane water electrolysis technology. J Huazhong Univ Sci Tech (Nat Sci Ed) 2023;51:111–22. https://doi.org/10.13245/j.hust.239016.
[47] Berrada A, Sanjari MJ, Mrabet RE. Techno-economic assessment of hydrogen production: comparative analysis of electrolyser technologies in a hybrid PV/wind system. Int J Hydrog Energy 2025;141:193–211. https://doi.org/10.1016/j.ijhydene.2025.05.384.
[48] Fabianek P, Madlener R. Techno-economic analysis and optimal sizing of hybrid PV-wind systems for hydrogen production by PEM electrolysis in California and northern Germany. Int J Hydrog Energy 2023. https://doi.org/10.1016/j.ijhydene.2023.11.196.
[49] Hill SJP, Bamisile O, Hatton L, Staffell I, Jansen M. The cost of clean hydrogen from offshore wind and electrolysis. J Clean Prod 2024;445:141162. https://doi.org/10.1016/j.jclepro.2024.141162.
[50] Arias I, Battisti FG, Romero-Ramos JA, Pérez M, Valenzuela L, Cardemil J, et al. Assessing system-level synergies between photovoltaic and proton exchange membrane electrolyzers for solar-powered hydrogen production. Appl Energy 2024;368:123495. https://doi.org/10.1016/j.apenergy.2024.123495.
[51] NASA Prediction of Worldwide Energy Resources (POWER). https://power.larc.nasa.gov/data-access-viewer/.
[52] Proost J. State-of-the art CAPEX data for water electrolysers, and their impact on renewable hydrogen price settings. Int J Hydrog Energy 2019;44:4406–13. https://doi.org/10.1016/j.ijhydene.2018.07.164.
[53] Chen Q, Gu Y, Tang Z, Wang D, Wu Q. Optimal design and techno-economic assessment of low-carbon hydrogen supply pathways for a refueling station located in Shanghai. Energy (Oxford) 2021;237:121584. https://doi.org/10.1016/j.energy.2021.121584.
[54] Tan Q, Mei S, Ye Q, Ding Y, Zhang Y. Optimization model of a combined wind–PV–thermal dispatching system under carbon emissions trading in China. J Clean Prod 2019;225:391–404. https://doi.org/10.1016/j.jclepro.2019.03.349.
[55] Zhou Z, Zheng M, Dong B, Li J. Cluster allocation strategy of multi-electrolyzers in wind-hydrogen system considering electrolyzer degradation under fluctuating operating conditions. Renew Energy 2025;242:122381. https://doi.org/10.1016/j.renene.2025.122381.
[56] Zou P, Lin H, Zhou X, Zou Y, Li Y, Yan G, et al. Control strategies for multi-electrolyzer alkaline hydrogen generation systems improving renewable energy utilization and electrolyzer lifespan. Renew Energy 2025;253:123628. https://doi.org/10.1016/j.renene.2025.123628.
[57] Ao Y, Zhu L, Xu Y, Li W, Zhao K, Yu Y. Operation strategy optimization of wind hydrogen electrolysis system considering degradation and price fluctuation. Renew Energy 2025;253:123449. https://doi.org/10.1016/j.renene.2025.123449.
[58] Zhang Q, Xie Di, Zeng Y, Liu Y, Yu H, Liu S. Optimizing wind-solar hydrogen production through collaborative strategy with ALK/PEM multi-electrolyzer arrays. Renew. Energy 2024;232:121116. https://doi.org/10.1016/j.renene.2024.121116.
[59] Wang T, Wang K, Wang Y, Shi F, Zhang Y. Mapping the concentrated solar power development in China: navigating brief challenges and embracing a bright future. Sustain Energy Technol Assess 2025;75:104228. https://doi.org/10.1016/j.seta.2025.104228.
[60] Si L, Wang P, Cao D. Towards sustainable development goals: assessment of wind and solar potential in Northwest China. Environ Res 2024:118660. https://doi.org/10.1016/j.envres.2024.118660.
[61] Liu F, Sun F, Wang X, Feng Y. Water constraints challenge large-scale solar expansion in Northwest China. Energy (Oxford) 2025:138288. https://doi.org/10.1016/j.energy.2025.138288.